Pacific Northwest
NATIONAL LABORATORY

PNNL-31881

Silicon-Based Anodes for Long-Cycle-Life Lithium-ion Batteries

August 2021

Jason Zhang
Qiuyan Li
Xiaolin Li
Wu Xu
Ran Yi

U.S. DEPARTMENT OF ENERGY

Prepared for the U.S. Department of Energy
under Contract DE-AC05-76RL01830

DISCLAIMER

This report was prepared as an account of work sponsored by an agency of the United States Government. Neither the United States Government nor any agency thereof, nor Battelle Memorial Institute, nor any of their employees, **makes any warranty, express or implied, or assumes any legal liability or responsibility for the accuracy, completeness, or usefulness of any information, apparatus, product, or process disclosed, or represents that its use would not infringe privately owned rights**. Reference herein to any specific commercial product, process, or service by trade name, trademark, manufacturer, or otherwise does not necessarily constitute or imply its endorsement, recommendation, or favoring by the United States Government or any agency thereof, or Battelle Memorial Institute. The views and opinions of authors expressed herein do not necessarily state or reflect those of the United States Government or any agency thereof.

PACIFIC NORTHWEST NATIONAL LABORATORY
operated by
BATTELLE
for the
UNITED STATES DEPARTMENT OF ENERGY
under Contract DE-AC05-76RL01830

Printed in the United States of America

Available to DOE and DOE contractors from the Office of Scientific and Technical Information,
P.O. Box 62, Oak Ridge, TN 37831-0062
www.osti.gov
ph: (865) 576-8401
fax: (865) 576-5728
email: reports@osti.gov

Available to the public from the National Technical Information Service
5301 Shawnee Rd., Alexandria, VA 22312
ph: (800) 553-NTIS (6847)
or (703) 605-6000
email: info@ntis.gov
Online ordering: http://www.ntis.gov

PNNL-31881

Silicon-Based Anodes for Long-Cycle-Life Lithium-ion Batteries

August 2021

Jason Zhang
Qiuyan Li
Xiaolin Li
Wu Xu
Ran Yi

Prepared for
the U.S. Department of Energy
under Contract DE-AC05-76RL01830

Pacific Northwest National Laboratory
Richland, Washington 99354

1. Introduction

Silicon (Si) has been regarded as one of the most promising anode materials for next generation lithium-ion batteries (LIBs) with high energy density because it has 10 times higher theoretical specific capacity (4200 mAh/g) than that of graphite. However, severe volume change (~300%) of Si during lithiation and delithiation hinders the practical application of Si anode. In most of literature report, nano Si was deposited on different graphite structures. One of the common features of these materials is that their nano Si is exposed to electrolyte and has large surface area. In the cased of carbon-coated SiO, first cycle efficiency of the anode if typically, less than 75%. In all these cases, Si or SiO will continue to react with electrolyte chemically or electrochemically (through leak current) even at open circuit conditions. We believe this is the origin of the shortened calendar life in the state-of-the-art Li ion batteries using Si based anode. Porous Si has been explored as a solution to large volume change as the void provides a buffer zone for Si expansion. To date, all of Si based Li ion batteries developed by industry still has a calendar lifetime of less than two years which is far less than 10 year target required by DOE (https://www.energy.gov/eere/vehicles/2020-vehicle-technologies-office-amr-presentations-program). Therefore, a solution to this problem has been regarded as one of the main goals in the field and is urgently needed by DOE.

2. Experiments and Results

The typical porous Si was generated by high temperature (850-1150°C) disproportion reaction of micron sized SiO precursor to form a composite of SiO_2 and Si with nano sized structures. Then HF etching is commonly used to prepare remove SiO_2. The surface of porous Si after HF etching is terminated with H as shown in Fig. 1a. However, H terminated Si is not stable and is prone to oxidation in air at room temperature, making storage of porous Si difficult. Also, Si-H bond will undergo cleavage upon heating, leaving Si radicals and as a result facilitating sintering of porous Si. In some of the prior art, porous Si has been soaked with carbon precursors at room temperature to ensure the complete penetration of the precursor. However, the penetrated gaseous precursor will not form a stable bond with Si surface at a temperature less than 100°C and is less effective in preventing shrinking of porous Si at high temperatures (> 400°C).

Several pre-treatment approaches that performed at a temperature far below the sintering temperature (~ 400°C) of porous Si and form an intermediate layer on inner pores of porous Si to stabilize Si during the subsequent high temperature treatment process. These processes are different from the Wang (US patent 9269949 B2, Feb. 23, 2016, Donghai Wang, Ran Yi, Fang Dai) and other prior art that did not form a stable intermediate coating layer on the inner surface of porous Si before carbonization process that leads to more sintering of Si. In one approach, a wet chemical process is used to coat carbon containing precursor to inner wall of nano pores of porous Si. The process starts at room temperature. Once the inner pore of porous Si is covered with a liquid phase of carbon-containing precursor in this low temperature process, porous Si will be much more stable during the subsequent carbonization process at elevated temperatures and the sintering of porous Si can be minimized. The carbon-containing solutions such as certain polymers can be introduced into the porous Si structure by infiltration under vacuum and form a coating throughout the porous Si. This step will be done at low temperature without intentional heating to avoid sintering of porous Si. The polymers will be converted to carbon coating on Si at elevated temperatures. During carbonization, sintering of porous Si will be minimized due to limited surface diffusion by carbon coating, which helps preserve porosity of the Si-C structure. A final carbon coating may be used to further block surface pores to eliminate possible electrolyte penetration into inside porous structure.

In another approach, a gaseous treatment process is used to coat carbon containing precursor to inner wall of nano pores of porous Si as shown in Fig. 1b-1c. This process can passivate H terminated Si by introducing a surface coverage of Si surface with hydrocarbon ligands at an elevated temperature which is high enough to initiate formation of new bound between carbon precursor and Si, but less enough to avoid sintering of Si. This passivation process can also be realized by solution phase treatment. The pretreatment process can form a stable Si-C covalent bond throughout the porous Si. This passivation layer will be converted to C in situ at the subsequent carbonization process and the sintering of porous Si will be minimized due to limited surface diffusion by Si-C covalent bond passivation, which helps preserve porosity of the Si-C structure.

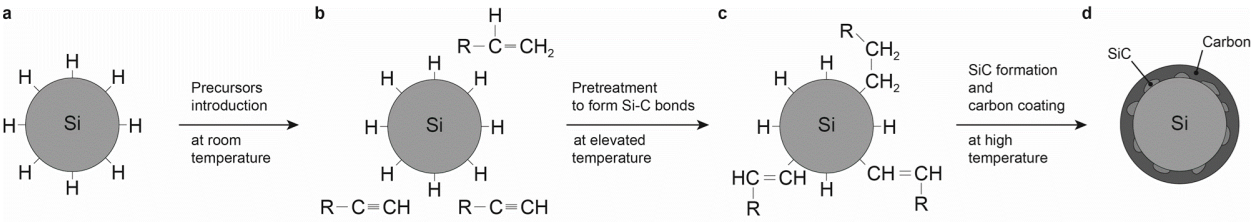

Figure 1. Scheme of porous Si before and after pretreatment.

To form the above structure, porous Si (prepared by heat treatment of SiO at 850°C in Ar atmosphere followed by HF etching to remove SiO_2) is pre-treated with phenylacetylene by infiltration of phenylacetylene into porous Si at 220°C for 1 hour to form a stable binding between carbon precursor and Si surface. Carbon coating of Si powder is carried out by CVD in a quartz tube at 700°C for 10 min using acetylene as carbon precursor. A new Si based porous structure (as shown in Figure 2) that features a SiC layer on Si, a carbon layer on SiC and sealed porosity. Intermediate layers of carbon containing precursors are chemically bonded to the inner pore of high surface area porous Si at a temperature much lower than those of Si sintering temperature. These ultra-thin (sub nm) intermediate layers can 1) form SiC layer and 2) passivate Si surface and minimize sintering of Si nano structure during the subsequent high temperature process, therefore enable the formation of a highly porous Si with SiC protection layer and carbon conductive network throughout the composite, ensuring a highly stable porous Si structure and high utilization of Si during charge/discharge process.

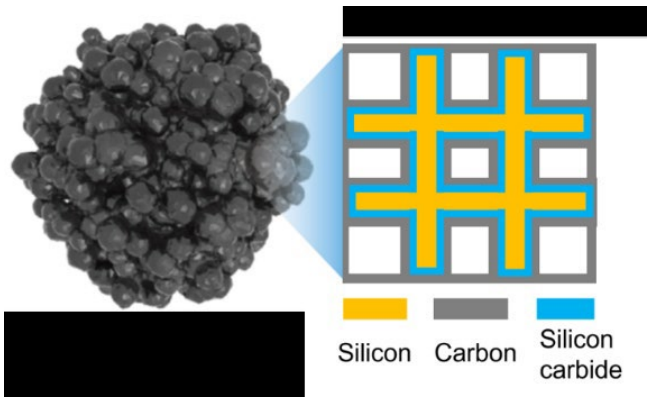

Figure 2. Scheme of structure of C/SiC/p-Si particles.

Figure 3 shows the cycling stability of the C/SiC/p-Si composite anode in a single layer pouch cell using $LiCoO_2$ as cathode and 1.2 M $LiPF_6$ in EC-PC-EMC (1:3:6 by wt) + 1 wt% VC + 7 wt% FEC as electrolyte. The cells are charged/discharged within a voltage window from 2.75 to 4.35V with 0.1C at the 1st cycle, 0.2C at the 2nd cycle and 0.5C (discharge)/0.7C (charge) thereafter. A capacity check cycle is done at every 50 cycles at 0.2C. No capacity fading is observed in Si||$LiCoO_2$ pouch cell. It is clear from

Figure 3 that the C/SiC/p-Si composite anode has excellent cycling stability with Si protected by both SiC and carbon in this unique structure design.

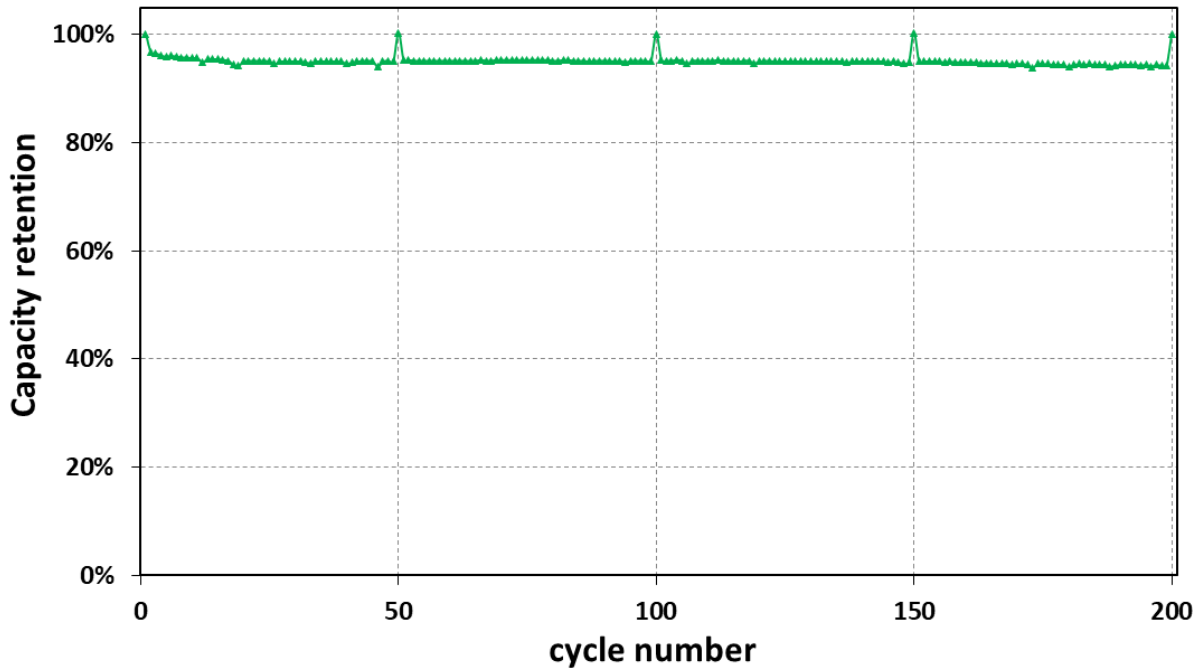

Figure 3. Cycling stability of the C/SiC/p-Si composite. (a) Capacity retention as a function of cycle number in half cell. (b) Coulombic efficiency as a function of cycle number in half cell. (c) Capacity retention as a function of cycle number in a Si||LiCoO2 pouch cell.

The goals of this work are 1) 2X scale up of porous Si anode materials using current CVD system; 2) tailoring electrolytes to enable long term cycling stability and good calendar life of porous Si-containing lithium ion batteries; and 3) pouch cell fabrication and testing. The details of these tasks and experimental results are summarized below.

2.1 Scale up on the Preparation of porous Si powder

Prior to the project, about 1.2g carbon coated porous Si could be prepared per each CVD batch. In this project, 2.6 g carbon coated porous Si per batch has been achieved with similar performance, which provides enough materials for electrolyte optimization and pouch cell fabrication and testing. In the meanwhile, more fundamental understanding on this material has been gained, which will serve as guidance for further scale up.

As the amount of porous Si increases, flow rate or/and CVD time of C_2H_2 (which is the carbon source for carbon coating) will need to be increased accordingly to reach the target carbon content. Various challenges have been encountered and overcome.

2.1a Process development to achieve 2X scale up—role of CVD temperature
The carbon coating by C_2H_2 decomposition is a highly exothermic reaction with a significant amount of heat generation. Increasing amount of porous Si precursor leads to an increase in absolute amount of heat generated and thus the rise of local temperature of Si during CVD. Because Si can react with carbon to form SiC at high temperature, the increase in temperature may cause formation of SiC. Although trace

amount of SiC contributes to improved protection of Si/electrolyte interface, excess SiC is not favorable since it is electrochemical inactive leading to lower overall capacity and it has low electrical conductivity leading to lower rate compatibility of final products. It has been found that keeping CVD temperature for 2X scale the same as 1X baseline indeed causes a large drop in capacity, indicating excess formation of SiC (N1 1x vs N1 2x LS1), as shown in the table below. Lowering the temperature results in similar capacity (N1 1x vs N1b 2x LS1), which suggests that a lower temperature is needed to prevent formation of SiC for scale up.

Table 1. Influence of CVD temperature of properties of N1 materials

Sample	N1 1x		N1 2x LS1		N1b 2x LS1	
Input (g)	0.7544		1.5441		1.5123	
Output (g)	1.2985		2.6792		2.7653	
Carbon mass (g)	0.5441		1.1351		1.253	
Carbon content	**41.90%**		**42.40%**		**45.31%**	
True density N2 (g/cm^3)	2.47		2.19		2.1	
Surface area (m^2/g)			3.64		6.66	
Pore volume (cm^3/g)			0.022		0.026	
1st lithiation capacity (mAh/g)	2084	2142	1898	1892	1938	1991

2.1b Process optimization to achieve clean CVD

Although lowering CVD temperature leads to similar properties of 2X N1 material, the process is not clean with carbon soot coated on the CVD tube due to high concentration of C2H2 used. This is not favorable because cleaning the tube requires downtime of the system. Two approaches have been studied to reduce the carbon soot contamination.

a. Role of CVD pressure

The reason for carbon soot formation is that there is excess carbon species that cannot be consumed by coating on Si, and they tend to react with each other to form free carbon—carbon soot. Since pressure is related to the concentration of a gas, lowering pressure could reduce the concentration and thus avoid carbon soot formation. However, a delicate balance is needed because a too low a pressure or gas concentration may not be enough to effectively form carbon coating on Si. In table 2 below, using a pressure of 70 torr does create a clean process without carbon contamination on the tube; however, the material has open structure after CVD even with longer CVD time as suggested by its high true density (see first two columns). An open structure after CVD is not desired because it promotes more electrolyte decomposition, lowering 1$_{st}$ cycle efficiency. Increasing the pressure to 110 torr leads to both a clean process and closed structure of final products. This result suggests that the pressure setting should be high

enough to ensure enough carbon species for carbon coating and at the same time low enough to avoid soot formation.

Table 2. Role of CVD pressure

Sample	**N1b3** 2x LS1-**70torr**-15min	**N1b3** 2x LS1-**70torr-25min**	**N1b4-110torr** 2x LS1
Input (g)	1.5198	1.5228	1.5152
Output (g)	2.5627	2.6914	2.685
Carbon mass (g)	1.0429	1.1686	1.1698
Carbon content	**40.70%**	**43.42%**	**43.57%**
True density N2 (g/cm^3)	-	-	3.2 (2.18 vs He) (3.1 ground and sieve)

2b. Role of carrier gas

Alternatively, the concentration of carbon species can be diluted by using inert carrier gases. Table 3 below shows the role of Ar gas. Ar is introduced with a specific flow rate to keep the partial pressure of C2H2 at 110 torr in the mixture. A similarly clean process is obtained with the dilution by Ar. This suggests that the use of carrier gas is effective to prevent carbon soot formation as long as the partial pressure of C2H2 is properly maintained during CVD.

Table 3. Role of carrier gas

Sample	**N1b4-Ar** 2x LS1 (C_2H_2 partial pressure 111 torr)	**N1b4-110 torr** 2x LS1
Input (g)	1.4821	1.5152
Output (g)	2.6767	2.685
Carbon mass (g)	1.1946	1.1698
Carbon content	**44.63%**	**43.57%**
True density N2 (g/cm^3)	3.3 (4.6 ground and sieved)	3.2 (2.18 vs He) (3.1 ground and sieve)

In summary, CVD process has been studied and optimized to achieve 2x scale up of porous Si anode materials with a clean process. The roles of CVD temperature, duration, C_2H_2 gas pressure, and carrier gas have been studied. It has been found that:

a. CVD temperature needs to be reduced as the amount of porous Si input increases to avoid excess heat generation and SiC formation during CVD.

b. C_2H_2 pressure needs to be set at a proper level to ensure enough carbon species for carbon coating while preventing carbon soot formation.

c. Elongating CVD time when the C_2H_2 gas pressure is too low is not effective for formation of closed structure.

d. Use of carrier gas is effective to prevent carbon soot formation.

These findings will serve as baselines to guide further scale up by CVD process.

2.2 Tailor electrolyte for Si based Li ion batteries

This task will tailor localized high concentration electrolyte (LHCE) for N1 Si based Li ion batteries. Electrolytes with suitable additives are investigated in the high voltage batteries based on high Si content anode. The formulations of the LHCEs (LHCE-1, LHCE-2, LHCE-3 and LHCE-4) and the conventional $LiPF_6$/carbonate electrolyte (1.2 M $LiPF_6$ in PC-EMC (3: 7 by wt.) + 1 wt.% VC + 7% wt.% FEC) for Si based batteries (noted as Si-baseline) are studied in this work.

Table 4. Electrolyte formulations of the baseline electrolyte for Si electrode and the four LHCEs studied

Electrolyte Code	Electrolyte formula
Si-baseline	1.2 M $LiPF_6$ in PC-EMC (3: 7 by wt.) + 1 wt.% VC + 7% wt.% FEC
LHCE-1	1.4 M LiFSI in DMC-EC-TTE
LHCE-2	1.4 M LiFSI in DMC-EC-FEC-TTE
LHCE-3	1.4 M LiFSI in DMC-FEC-TTE
LHCE-4	1.4 M LiFSI in DMC-EC-FEC-TTE

The long-term cycling of these LHCEs and the Si-baseline were investigated in Si||NMC622 coin cells under the voltages range of 2.0 - 4.35 V and a charge rate of 0.7C and a discharge rate of C/2 after two formation cycles performed at C/10 for the first cycle and C/5 for the second cycle, where 1C = 3 mAh cm-2. Si anode is pre-lithiated with 30% capacity. Figure 4 shows the specific capacity over the long-term cycling using different electrolytes. For the Si-baseline, the cell is stable for around 350 cycles and starts a fast decay after 350 cycles, with capacity retentions of 82.6% and 26.0% at the 350th and 600th cycles, respectively (compared to the capacity of the first cycle at C/3 rate after the two formation cycles). This can be attributed to the poor electrode/electrolyte stability of Si-baseline electrolyte on both Si and NMC622, which leads to a quick accumulation of resistive surface films on Si and NMC622. In comparison, it is clearly observed that the three LHCEs (LHCE-1, LHCE-3 and LHCE-4) have much higher capacity retention in Si||NMC622 than the Si-baseline electrolyte. The cells with LHCE-1, LHCE-3 and LHCE-4 give discharge capacities of 155.0, 144.5 and 145.8 mAh g-1 at the 500th cycle with capacity retentions of 83.8%, 77.5% and 79.1%, respectively.

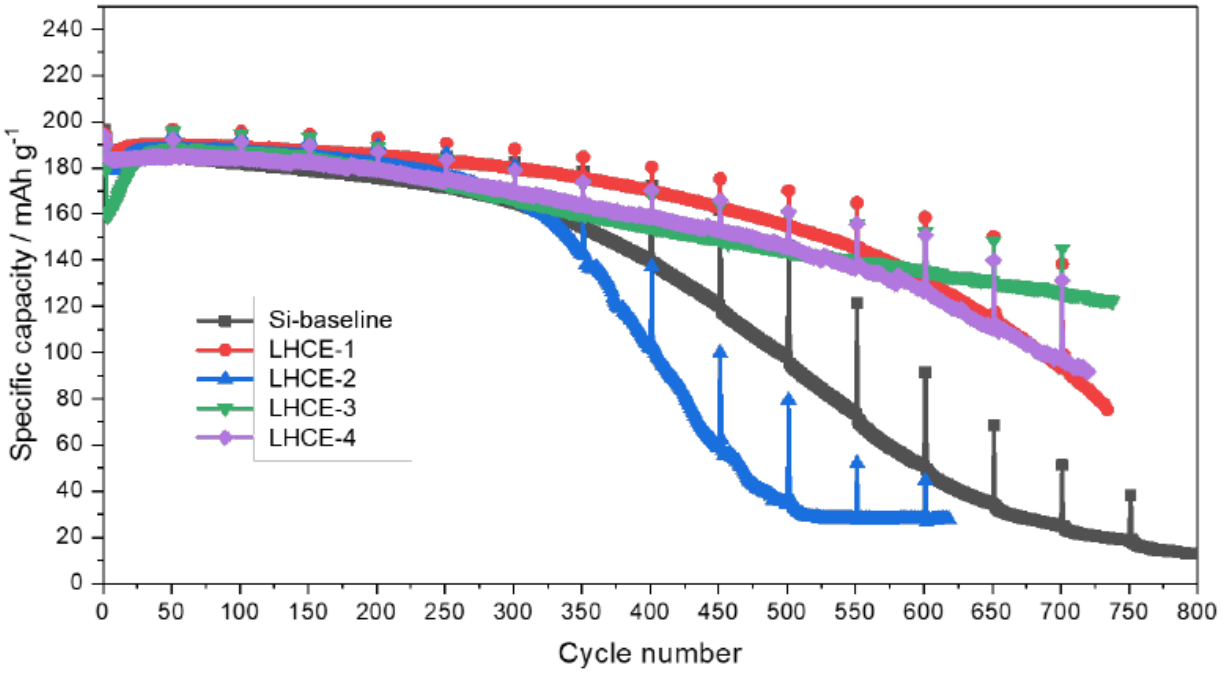

Figure 4. Long-term cycling (specific capacity) of Si||NMC622 coin cells with different electrolytes at 25 °C at 0.7C charge and C/2 discharge after formation cycle of C/10 in the 1st cycle and C/5 for the 2nd cycle. Capacity check at C/5 at every 50 cycles. Si with 30% capacity pre-lithiation

Figure 5 shows the corresponding CEs during the long-term cycling as shown in Figure 4. All the cells show high average CE above 99.8% during the cycling, and the detailed values are summarized in Table 4. One interesting phenomenon is the CE fluctuation during the C rate change at every 50 cycles, where C/5 charge/discharge is used for capacity check. Much higher CE fluctuation of 60% after long term cycling is observed in Si||NMC622 cells with Si-baseline and LHCE-2 electrolytes, where the fluctuation significantly increases after 350 cycles, which is in consistent with the fast capacity decay after 350 cycles in these two electrolytes. Electrolytes LHCE-1, LHCE-3 and LHCE-4 have much smaller CE fluctuation within 10% after 500 cycles. These results tell that the cells using optimized LHCEs have much lower resistance and better kinetics after long term cycling, which can be attributed to the significantly improved SEI and CEI properties on Si anode and NMC622 cathode cycled in such LHCEs.

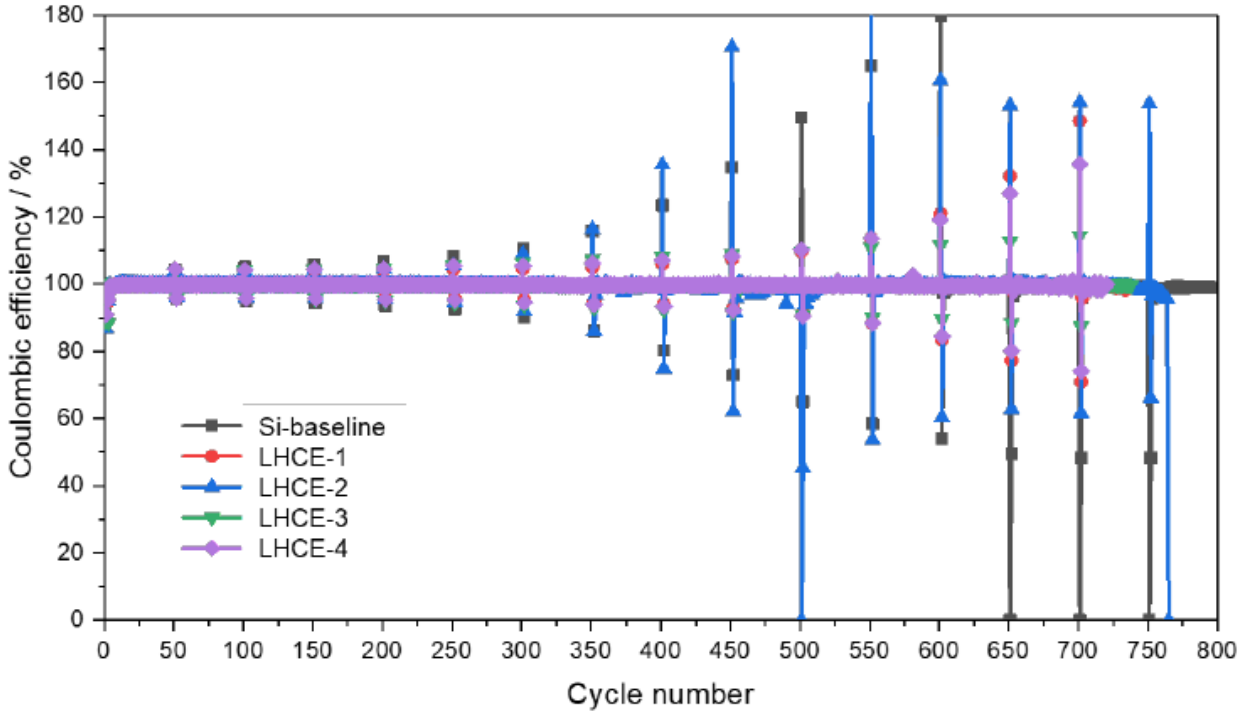

Figure 5. Long-term cycling (Coulombic efficiency) of Si||NMC622 coin cells with different electrolytes at 25 °C at 0.7C charge and C/2 discharge after formation cycle of C/10 in the 1st cycle and C/5 for the 2nd cycle. Capacity check at C/5 at every 50 cycles. Si with 30% capacity pre-lithiation

Table 4. First cycle Coulombic efficiency (FCE) and average Coulombic efficiency (ACE) during cycling of the Si-baseline electrolyte and the four LHCEs studied

	25 °C (Si with 30% pre-lithiation)		**45 °C (Si without pre-lithiation)**	
Electrolyte	**FCE / %**	**ACE / %**	**FCE / %**	**ACE / %**
Si-baseline	91.05	99.84	84.88	98.90
LHCE-1	90.94	99.88	84.57	99.81
LHCE-2	86.84	99.72	83.59	99.8
LHCE-3	88.87	99.89	84.99	99.84
LHCE-4	91.02	99.81	85.03	99.81

The voltage profiles of selected cycles during cycling are given in Figure 6, where LHCE-1 represents the optimized LHCE and Si-baseline is compared as a reference. For the cell using Si-baseline, the overpotential increases significantly upon cycling with a 0.6 V increase from the 3rd cycle (first cycle after 2 formation cycles) to 500 cycles, evidenced the large resistance increase during cycling. However, for the cell using LHCE-1 electrolyte, the overpotential at initial charge state barely changed during long-term cycling, suggesting a much small change of resistance.

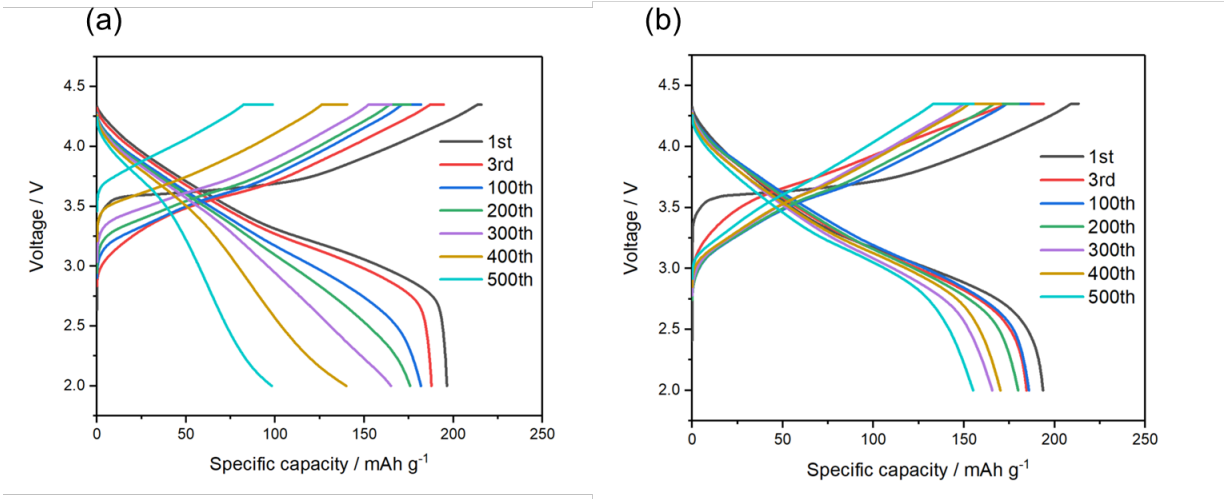

Figure 6. Voltage profiles of Si||NMC622 coin cells using different electrolytes (a) Si-baseline and (b) LHCE-1 at 25 °C at 0.7C charge and C/2 discharge after formation cycle of C/10 in the 1st cycle and C/5 for the 2nd cycle. Capacity check at C/5 at every 50 cycles. Si with 30% capacity pre-lithiation.

In addition, Si||NMC622 cells were also tested at elevated temperature of 45 °C. To simplify the testing and be more practical, Si anode is not pre-lithiated in the Si||NMC622 cells tested at 45 °C. As shown in Figure 7, all four LHCEs show much stable cycling performance than that of the Si-baseline electrolyte, which shows clear capacity decay. The capacity retention for LHCE-1, LHCE-2, LHCE-3 and LHCE-4 after 500 cycles are 76.5%, 43.2%, 72.2% and 76.7% respectively, while it is 11.5% for the Si-baseline electrolyte after 300 cycles.

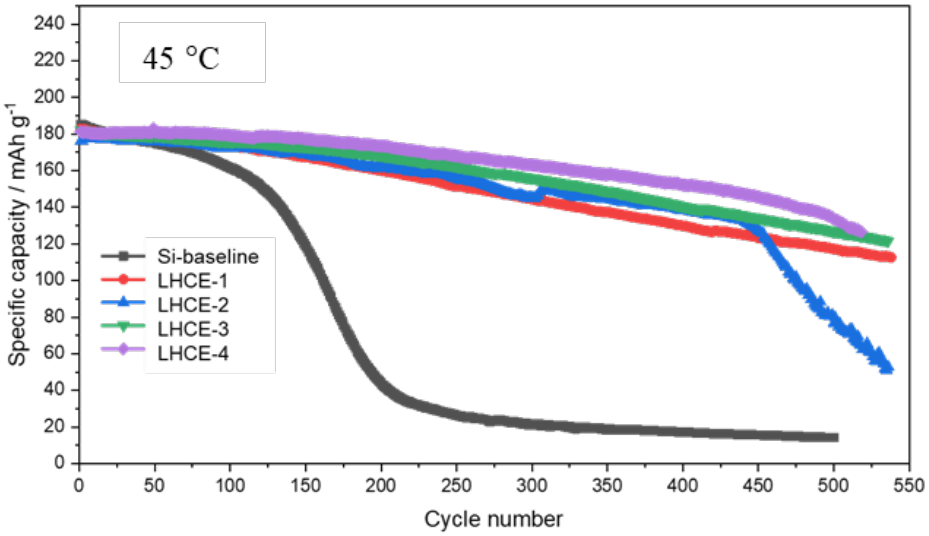

Figure 7. Long-term cycling (specific capacity) of Si||NMC622 coin cells with different electrolytes at 45 °C after formation cycles of C/10 in the 1st cycle and C/5 for the 2nd cycle at 25 °C. Capacity check at C/5 at every 50 cycles. Si is used without pre-lithiation.

The corresponding CE during the cycling at 45 °C is shown in Figure 5. All the cells with LHCE-1, LHCE-2, LHCE-3 and LHCE-4 show higher average CE above 99.8% during the cycling than 98.9% of Si-baseline, and the detailed values are summarized in Table 4. As the same to 25 °C, the CE fluctuation during the C rate change at every 50 cycles is smaller in the LHCEs, indicating the resistance of the

Si||NMC622 is smaller in the LHCES than the cell with Si-baseline electrolyte. The fast CE drop in the Si-baseline indicates the fast depletion of the active Li in the cells, while the CE of the cells with LHCEs are stable during cycling.

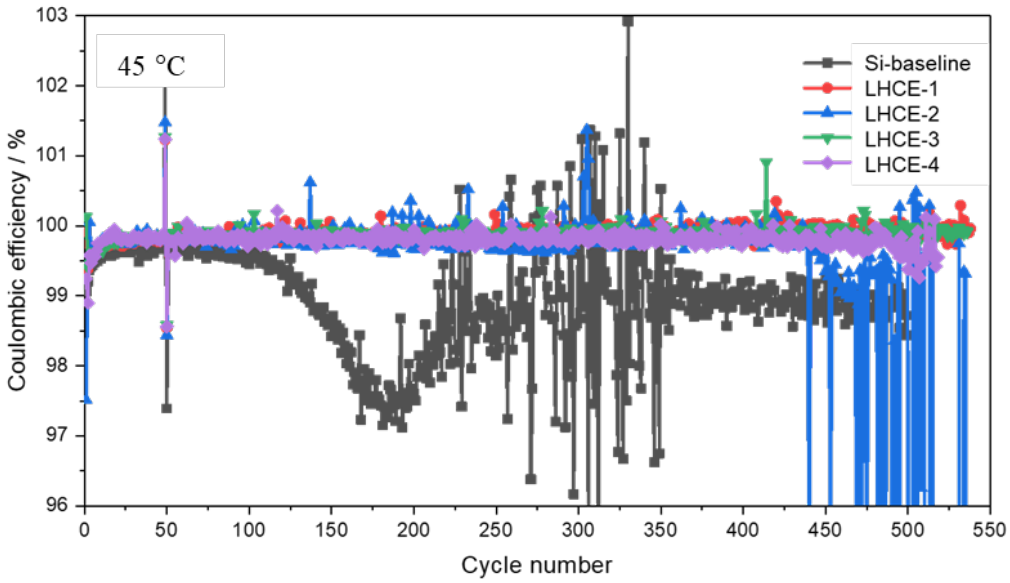

Figure 8. Long-term cycling (Coulombic efficiency) of Si||NMC622 coin cells with different electrolytes at 45 °C after formation cycle of C/10 in the 1st cycle and C/5 for the 2nd cycle at 25 °C. Si is used without pre-lithiation.

2.3 Calendar life testing in SLP for Si based anode

This task has prepared and tested multiple single layer pouch cells and perform calendar life test. The binder will also be tailored to improve the calendar life of the cells. Accelerated aging experiments are used to predict cell calendar life based on protocol used by USABC. The testing condition for calendar life is to store the cells with Si based materials at 100% SOC at four different temperatures (30 °C, 40 °C, 47.5 °C, and 55 °C). The cells are placed in an isothermal chamber and endures MPPC pulse every day for 32 days as a loop and HPPC protocol after a loop. From the MPPC test, discharge resistance is calculated by taking the difference between the initial voltage prior to the pulse and the voltage at the end of the pulse divided by the constant current. The capacity retention at C/3 is recorded after storage. Calendar life with different electrolytes were evaluated in the SLP based on high Si content anode.

The calendar life of Si||NMC622 SLP cells with LHCE-4 and the baseline electrolyte (Si-baseline-2) were investigated under the voltage range of 2.0 - 4.35 V and a charge rate of 0.7C and a discharge rate of 0.5C after two formation cycles performed at C/10 for the first cycle and C/5 for the second cycle, where 1C = 3.2 mAh cm-2. Si anode is pre-lithiated. Figure 9 shows the relative resistance over the long-term storage using different electrolytes. The performance of the cells using these two electrolytes at 30 °C and 55 °C are compared in Figure 10. For both electrolytes, the resistance is increased with increasing storage time and temperature. In N1 materials with the conventional LiPF6/carbonate electrolyte system, their resistance is increased by 100% after 32 days storage at 30 °C and 40 °C. When the temperature is elevated to 47.5 °C and 55 °C, the resistance is obviously boosted by 200%, the cells cannot endure this high temperature and voltage obviously drops during rest time so that self-discharge interrupts the resistance increase after 15 days. In Si||NMC622 SLP cells with the LHCE-4, their resistance increased 24% after 32 days storage at 30 °C. On the contrary, the resistance at 40 °C is lower than 30 °C, that is because the slight high temperature prompts the Li transportation in high concentration electrolyte but does not produce more by-product to increase the impedance, when temperature is elevated to 47.5 °C

and 55 °C, the accelerated side reaction between electrolytes and Si materials resulting in more and more accumulation of by-produce and impedance increase.

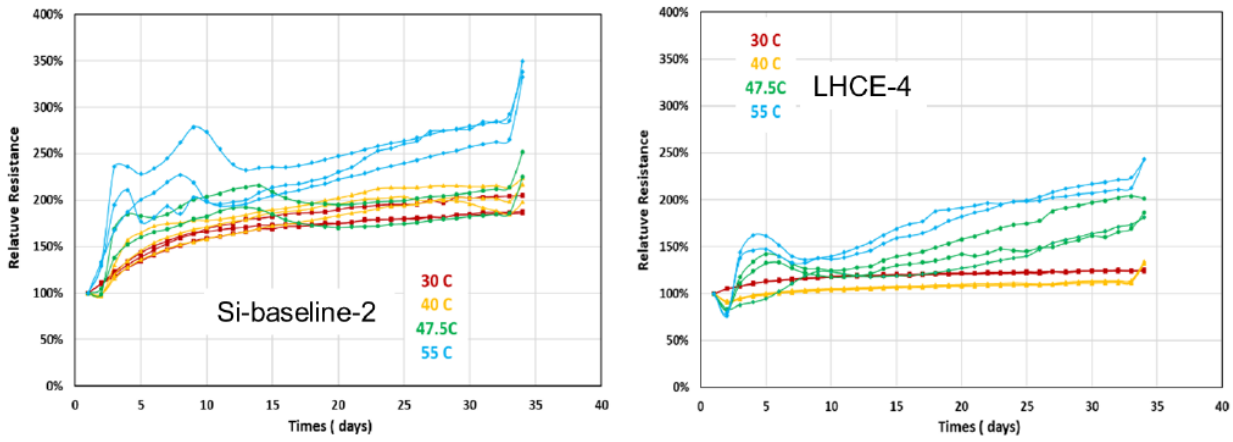

Figure 9. Calendar life testing (relative resistance) of Si||NMC622 SLP with different electrolytes (a) Si-baseline-2, (b) LHCE-4 at different temperatures.

Figure 10 compared the results of calendar life testing of Si||NMC622 SLP using Si-baseline-2 and LHCE-4. It can be seen that the SLP has only the initial resistance of 1.78 Ω with the conventional $LiPF_6$/carbonate electrolyte and 3.1 Ω with the LHCE-4 at 30 °C, respectively, the former significantly increases and the latter increases slowly during the storage, which indicts LHCE-4 can formed thick and good SEI on Si surface at the beginning and mitigates the further reaction with electrolyte during the storage. At 55 °C, high temperature plays a role in accelerating the reaction between Si materials and electrolyte, and the accumulated by-product increases the initial impedance in both systems, the difference of resistance is reducing during storage, gas generation and self-discharge and other factors can also contribute to impedance increase. That is why the more fluctuation was observed in resistance at 55 °C storage. It brings some error for the prediction of calendar life.

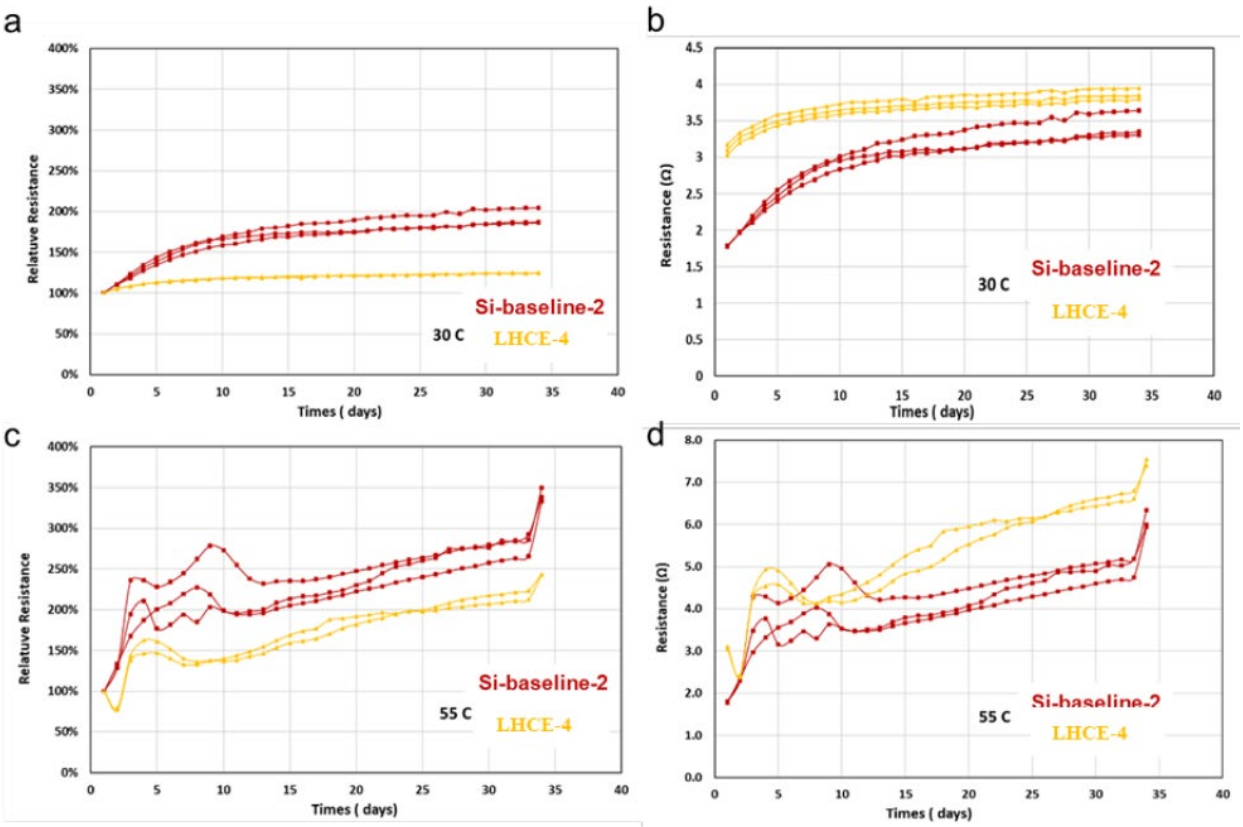

Figure 10. Calendar life test of Si||NMC622 SLP cells using Si-baseline-2 and LHCE-4 electrolytes. (a) and (c) are the relative resistance of the cells at 30 °C and 55 °C, respectively. (b) and (d) are the absolute resistance of the cells at 30 °C and 55 °C, respectively.

After storage, the residual capacity of the cells needs to be further checked to see if cell is healthy or failed. As showed in Table 5, the recovered capacity after storage of SLP with both the conventional LiPF6/carbonate electrolyte (Si-baseline-2) and the LHCE-4 at 30 °C and 40 °C has almost no change compared with the initial capacity before storage, which indicts all capacity is recovered after storage and the cell is healthy at this status although they shows 100% resistance increase. This means that the cell capacity has less correlation with this resistance even when the resistance increased by 24% to 100% in different electrolytes. With increasing temperature, less capacity can be recovered because more Li consumes with the reactions between Si and electrolyte during the high temperature storage, the SLPs with LHCE-4 and carbonate electrolyte still have 90% and 88% capacity retention respectively although they show very high relative resistance at this status. Hence, the healthy status and recovered capacity of cell must be considered as criteria for the prediction of calendar life base on the relative resistance.

Table 5. Capacity retention after storage at different temperatures

Capacity retention after storage/ before storage at 0.33C			
		Si-baseline-2	LHCE-4
30 °C	Cell 1	100%	99%
	Cell 2	102%	98%
40 °C	Cell 1	104%	106%
	Cell 2	108%	106%
47.5 °C	Cell 1	97%	82%
	Cell 2	90%	87%
55 °C	Cell 1	91%	91%
	Cell 2	86%	90%

3. Conclusion

In summary, CVD process has been studied and optimized to achieve 2x scale up of porous Si anode materials with a clean process. The roles of CVD temperature, duration, C_2H_2 gas pressure, and carrier gas have been optimized. It is found that LHCE (LHCE-1 and LHCE-4) can lead to more than 50% increase in the cycling stability of Si||NMC622 cells. LHCE-4 can also lead to smaller impedance increase and longer calendar life when tested in single layer pouch cells. These results are very helpful in the understanding of the Si based anode and further development of Si based Li ion batteries.

Publications/presentations/Patent applications:

1. Highly-Stable Li Ion Batteries Based on Porous Si Anode and Localized High Concentration Electrolytes, Ran Yi, Sujong Chae, Qiuyan Li, Xiaolin Li, Wu Xu, and Ji-Guang Zhang,* presented in 238th ECS meeting, Oct. 6, 2020.
2. Wu Xu et al., Electrolytes for Lithium Ion Batteries with Graphite and/or Silicon Anodes, U.S. provisional patent application filed on 9/2020.

Pacific Northwest National Laboratory

902 Battelle Boulevard
P.O. Box 999
Richland, WA 99354
1-888-375-PNNL (7665)

www.pnnl.gov